

1 **Neutron Optics Optimization for the SNS EQ-SANS Diffractometer**

2

3 **Jinkui Zhao**

4 Neutron Scattering Sciences Division, Oak Ridge National Laboratory, Oak Ridge, TN

5 37831, USA

6

7 **Abstract**

8 The extended Q -range small angle neutron scattering (EQ-SANS) diffractometer at the
9 Spallation Neutron Source has recently been completed. Initial commissioning has shown
10 that it has achieved its high intensity, low background, and wide dynamic range design
11 goals. One of the key components that enable these performances is its neutron optics,
12 which are extensively optimized using analytical and Monte Carlo methods. The EQ-
13 SANS optics consist of a curved multichannel beam bender and sections of straight
14 neutron guides on both ends of the bender. The bender and the guide are made of float
15 glass coated with supermirror multilayers. The function of the optics is to ensure low
16 instrument background by avoiding the direct line of sight of the neutron moderator at
17 downstream locations, while transporting thermal and cold neutrons to the sample with
18 maximum efficiency. In this work, the optimization of the EQ-SANS optics is presented.

19

20 **Keywords** Neutron optics, multichannel beam bender, SANS, Spallation Neutron Source,
21 Monte Carlo Simulations.

22

23 **1. Introduction**

24 One of the major design challenges of a high performance small angle neutron scattering
25 (SANS) diffractometer on a spallation neutron source is how to maximize neutron flux on
26 sample and minimize instrument background in the same time. The difficulty is
27 especially great when the repetition rate of the source is high. When the rep rate is high,
28 the length of a SANS instrument has to be short in order for the instrument to have a wide
29 wavelength band, which is needed to increase the total neutron flux on sample. On the
30 other hand, a short instrument complicates background shielding. Spallation neutron
31 sources produce large amounts of fast neutrons at time zero, namely at the time when an
32 accelerated proton pulse strikes the target and a neutron pulse is generated (prompt pulse).
33 These fast neutrons are a main source of instrument background. Due to their very high
34 energy, shielding against them is extremely difficult. One novel approach in new
35 generations of SANS diffractometers is to use multichannel beam benders to change the
36 direction of thermal and cold neutrons and to get away from the direct line of sight from
37 the neutron moderator (i.e. neutron source). Many meters of shielding materials,
38 commonly steel and concrete, are then stacked after the last direct-line-of-sight point to
39 block these fast neutrons. The flight direction of fast neutrons cannot be bent by the beam
40 bender. The newly commissioned EQ-SANS diffractometer [1] at the Spallation Neutron
41 Source (SNS) is one such instrument. Its optics use a combination of a multichannel
42 beam bender and straight neutron guides. The last direct line of sight from the moderator
43 on the instrument is ~6m upstream from the sample, allowing ample amount of shielding
44 spaces. The optics transport thermal and cold neutrons with very high efficiency, making
45 it possible for the EQ-SANS instrument to achieve its high performance.
46

47 **2. Design Summary**

48 Figure 1 shows the schematic presentation of the EQ-SANS beam optics. Figure 2 shows
49 photos of selected optical components. The optics has a beam cross section of $40 \times 40 \text{mm}^2$.
50 It starts in the core vessel insert of the SNS target station with a 270mm long steel
51 collimator, followed by a 1m long section of straight neutron guide. Located in the
52 primary beam shutter and the bulk shield insert of the SNS target station is a 3.3m long, 6
53 channel, curved beam bender. The bender follows an arc with the radius of 95m. Beyond
54 the bulk shield insert are $\sim 4\text{m}$ of straight neutron guides and two additional meters of
55 removable guides (the second meter is to be installed). The optics is manufactured by
56 SwissNeutronics Inc [2] with the following parameters: all of the benders and guides are
57 coated with supermirror multilayers with the critical reflection angle of $3.5 \times \theta_c$, except the
58 convex sides of the bender channels, which have $2\theta_c$ supermirrors (θ_c is the critical
59 reflection angle of natural nickel); the reflectivity is $\geq 70\%$ for the $3.5\theta_c$ coatings and $\geq 90\%$
60 for the $2\theta_c$ coatings.

61

62 **3. Design Optimization**

63 The EQ-SANS diffractometer is intended to be a workhorse for the SNS. It is a short
64 instrument with 14m of primary flight path [1]. Because the instrument has pinhole
65 geometry and requires collimation space upstream from the sample, the fixed portion of
66 its optics is designed to terminate at 10m from the moderator. In the current work, the
67 optimization process for the EQ-SANS optics is constraint under this condition. In
68 addition, the width of the beam (40mm) is considered to be optimal for the EQ-SANS,
69 since its typical scattering samples are 20mm or less in size. Nonetheless, options for

70 higher beams are explored. The neutron beam is curved in the horizontal direction. So a
71 higher beam does not affect its bending. Other parameters that are optimized include the
72 number of bender channels, the radius of bender curvature, and the supermirror
73 multilayer coatings etc. The main optimization goal is to maximize the transport of
74 thermal and cold neutrons and to avoid the moderator direct line-of-sight as upstream
75 from the sample position as possible.

76

77 **3.1 Monte Carlo Simulation Conditions**

78 The parameters of the EQ-SANS optics as described in section 2 and figure 1 (without
79 the last two pieces of removable straight guides) are used as the baseline design for the
80 simulations and performance comparisons. Unless otherwise stated, a $40\times 40\text{mm}^2$
81 collimation slit and a $20\times 20\text{mm}^2$ sample slit are located at 10m and at 14m from the
82 moderator, respectively. The detector is located immediately after the sample slit. The
83 reflectivity for the supermirror coatings are set to 98% at θ_c , 90% at $2\times\theta_c$ for the convex
84 side of the bender walls, and 70% at $3.5\times\theta_c$ for the rest of the optics. The moderator
85 spectra are obtained from reference [3]. Neutrons are generated at the source with $\pm 1^\circ$
86 divergence, which is sufficient to fully illuminate the optical system with the 4m
87 collimation setting for the simulations. The simulations were performed using the Monte
88 Carlo program IB [4]. The statistics presented here corresponds to 10^{11} neutrons
89 generated at the neutron source and on the order of 10^8 neutrons detected at the sample
90 location.

91

92 **3.2 Bender versus Straight Guide**

93 Alternative to using a multichannel beam bender is to use a straight neutron guide in
94 combination with a T0 chopper. A T0 chopper is a large piece of dense material, such as
95 steel, that rotates into the neutron beam at time zero to block the fast neutrons and gamma
96 rays from the prompt neutron pulse. Figure 3 shows the simulated relative transmission of
97 the EQ-SANS optics as compared to a straight guide alternative. The transmission is
98 defined as the ratio of neutron counts at the sample location versus the number of
99 neutrons that enter the optics. The relative transmission is obtained from the transmission
100 of EQ-SANS optics divided by that of the straight guide alternative. For cold neutrons
101 with wavelength $\lambda > 5\text{\AA}$, the EQ-SANS optics and the alternative straight guide transport
102 neutrons with about the efficiency. Either of these two options will deliver about a 9×
103 flux gain when compared to no optics in the beam. The EQ-SANS optics thus offer the
104 instrument an excellent cold neutron performance. For shorter wavelength neutrons, the
105 straight guide option has a clear advantage. However, with the straight guide, the
106 operation and maintenance of the required T0 chopper is very burdensome. Even with a
107 lower optical transmission for short wavelength neutrons, the flux on sample at these
108 wavelengths on the EQ-SANS is still sufficiently high (figure 3) to allow the instrument
109 to effectively extend its neutron momentum transfer (Q) coverage to larger Q -values.

110

111 **3.3 First Section of Guide**

112 Since the EQ-SANS diffractometer is a short instrument, its optics need to be close to the
113 source in order for the instrument to avoid the moderator direct line of sight early on.

114 Energy deposition calculation and thermal analysis have predicted that, after a short piece
115 of collimator (figure 1), neutron optics can indeed start within the core vessel insert of the

116 SNS target station without significant risks of being damaged by the neutron source [5,6].
117 Nonetheless, placing a multichannel beam bender inside the core vessel still carries some
118 operational risks, since a damaged beam bender may render the instrument unusable.
119 Therefore, the EQ-SANS optics starts with a 1m long straight guide (figure 1). This guide
120 section increases the flux on sample by as much as 20% when compared with the case
121 where the guide is replaced with a collimator (figure 4). Opening up the collimator to
122 allow the multichannel beam bender that follows (figure 1) to have a full view of the
123 neutron moderator can achieve the same flux gain, but at the expense of shifting the
124 direct line of sight of the moderator further downstream, creating more burden for
125 background shielding.

126

127 **3.4 Bender Length, Radius, and Number of Channels**

128 The length of the multichannel beam bender (3.3m) is largely constraint by the physical
129 dimensions of the primary beam shutter and the bulk shield insert of the SNS target
130 station. On the downstream end of the bender, the first bandwidth chopper is located in
131 the target station's chopper cave on the perimeter of the target monolith (figure 1, [1]).
132 Extending the bender beyond this first bandwidth chopper is possible. However, spanning
133 multichannel benders across a bandwidth chopper creates concerns for accurate
134 alignment. In addition, benefit of a longer bender can also be obtained from optimizing
135 other bender parameters, such as the bender curvature and the number of channels.

136

137 The radius of curvature and the number of channels first and foremost affect the bender
138 transmission for short wavelength neutrons. With a larger radius ($R=150\text{m}$, figure 5) or

139 more channels (10 channels, figure 5), for example, the bender performance increases for
140 $< 2\text{\AA}$ neutrons. However, each of these options has a disadvantage. A larger bender radius
141 pushes the last direct line of sight of the moderator further downstream. More channels
142 mean that more materials in the beam to attenuate the flux, especially for cold neutrons.
143 The thinnest non-borated glass that was available as bender inserts for the EQ-SANS
144 optics is $\sim 0.55\text{mm}$ thick [1].

145

146 **3.5 Supermirror Coating**

147 Supermirror multilayers with large critical reflection angles and high reflectivity are
148 essential for the performance of the EQ-SANS optics. This is evident from figure 6,
149 which shows the relative transmission of a Ni coated EQ-SANS optics ($1 \times \theta_c$). Within the
150 divergence limit set by the 4m collimation (see section 3.1), the Ni coated optics will
151 transport neutrons only effectively for $> 7\text{\AA}$ neutrons. The effect of the mirror reflectivity
152 is also demonstrated in figure 6. For the Ni simulation, the reflectivity at θ_c is assumed to
153 be 100%, which results in a better transmission for colder neutrons than the EQ-SANS
154 optics. The latter uses a reflectivity of 98% at θ_c for the simulation (see section 3.1).

155

156 The curved nature of the EQ-SANS bender means that the multilayer coatings on the
157 convex sides of the bender walls can have a smaller critical angle than the concave side.
158 In fact, with its $2\theta_c$ coating on the convex sides of the channels, the EQ-SANS optics has
159 a slightly better simulated transmission for $< 2.5\text{\AA}$ neutrons than if the bender were coated
160 with $3.5\theta_c$ multilayers on all sides (figure 6). Similar to the above discussion on Ni coated
161 guides, the difference arises from the fact that the $2\theta_c$ multilayers have a higher

162 reflectivity than the $3.5\theta_c$ coatings at the reflection angle of $2\times\theta_c$. Such difference may
163 not be significant for the actual bender due to variations in multilayer manufacturing. In
164 any event, replacing the convex side of the EQ-SANS bender with the much less
165 expensive $2\theta_c$ multilayers will not degrade its performance.

166

167 **3.6 Guide Height**

168 Because the EQ-SANS beam bender curves in the horizontal direction only, it is tempting
169 to look into options of having a higher beam cross section. A higher beam will not affect
170 the avoidance of the direct line of sight of the neutron moderator, but will bring more
171 neutrons toward the sample area. However, since the EQ-SANS has pinhole geometry,
172 the collimation and sample slits need to be either square or circular for most experiments.
173 Under such constraints, higher beam cross section for the optics will not benefit the flux
174 on sample (figure 7).

175

176 **4. Performance**

177 At the exit of the multichannel bender, the neutron flux is fairly evenly distributed for
178 cold neutrons (data not shown). This is not the case at shorter wavelength due to garland
179 reflections (figure 8). However, after the additional three sections of straight neutron
180 guides (figure 1), this unevenness becomes insignificant (figure 8).

181 For SANS instruments, the most important performance criterion for the optics is to
182 maximize the flux at the sample location and to minimize the instrument backgrounds
183 due to fast neutrons from the prompt pulse. Figure 9 shows the simulated and measured
184 fluxes on the EQ-SANS instrument constructed with the presented optics. The

185 comparisons are performed for two configurations: One is for the flux at the end of the
186 neutron guides with no collimation. The other is at the sample location, which is 4 m
187 away from the optics. It is apparent that the EQ-SANS optics perform largely as expected.
188 We note that the measured fluxes are ~25% lower than simulated ones. There are two
189 apparent factors that can contribute to this discrepancy. The as-built EQ-SANS optics
190 have 10 mm thick of vacuum window materials along the beamline. There are additional
191 4 mm of window materials from the beam monitor which is located at the end of the
192 neutron guides [1]. These 14 mm thick materials are made of aluminum alloys, which can
193 attenuate the neutron beam by ~10% for 5 Å neutrons and ~ 20% for 20 Å ones.
194 Additionally, the as-built optics will not have the perfect manufacturing, installation, and
195 alignment accuracies as were assumed in the simulations, further decreasing the flux at
196 the sample. These imperfections are also apparent in the spectra for short wavelength
197 neutrons, where the measured flux drops off faster than the simulations as the neutron
198 wavelength decreases. Because the neutron total reflection angle decreases with
199 wavelength, these imperfections will have more impact on neutrons with shorter
200 wavelength.

201

202 **Acknowledgements**

203 During the course of its design, the EQ-SANS instrument and its optics have gone
204 through numerous reviews. The author is grateful to all those who have offered useful
205 discussions and suggestions.

206 This manuscript has been authored by UT-Battelle, LLC, under Contract No. DE-AC05-
207 00OR22725 with the U.S. Department of Energy. The United States Government retains,

208 and the publisher, by accepting the article for publication, acknowledges that the United
209 States Government retains a non-exclusive, paid-up, irrevocable, world-wide license to
210 publish or reproduce the published form of this manuscript, or allow others to do so, for
211 United States Government purposes.

212

213 **References**

214 [1] J.K. Zhao, C. Y. Gao, and D. Liu "The Extended Q-Range Small Angle Neutron
215 Scattering Diffractometer at the SNS" *J. Appl. Cryst.* 43 (2010) 1068-1077.

216 [2] www.swissneutronics.ch.

217 [3] E. B. Iverson, P. D. Ferguson, F. X. Gallmeier, and I. I. Popova,"*Neutronics*
218 *calculations for scattering instrument design: SCT configuration*", SNS Document:
219 SNS-110040300-DA0001-R00, Oak Ridge, TN, USA, (2002).

220 [4] J.K. Zhao "*IB: a Monte Carlo Simulation Tool for Neutron Scattering Instrument*
221 *Design under Parallel Virtual Machine*". Submitted to NIM-A (2011).

222 [5] B. D. Murphy "*Extended Energy-Deposition and Damage Calculations in Core-*
223 *Vessel Inserts at the Spallation Neutron Source*" SNS Document: SNS-107030600-
224 DA0001-R01, Oak Ridge, TN, USA, April (2003).

225 [6] K. W. Childs "*Thermal Analysis of the 06td SANS Diffractometer Core Vessel Insert*
226 *and Guide*" SNS Document: SNS-107080600-DA0005-R00, Oak Ridge, TN, USA,
227 July (2003).

228

229 **Figure Captions**

230 Figure 1: Schematics of the optics system for the EQ-SANS instrument at the SNS. The
231 gaps between the straight neutron guides sections outside the SNS target monolith are
232 reserved for bandwidth choppers. The last two sections of the straight neutron guides are
233 removable, and the very last section is to be installed.

234

235 Figure 2: Photographs of the EQ-SANS core vessel insert guide (left) and a section of the
236 multichannel beam bender (right) in their respective steel casings.

237

238 Figure 3: Relative transmission of the EQ-SANS optics as compared to a straight guide
239 (left axis), and the simulated flux on sample with the EQ-SANS optics (right axis). For
240 the straight guide simulation, a 500mm gap is introduced in the optics to simulate the
241 effect of a T0 chopper. The straight guide has the same $3.5 \times \theta_c$ supermirror coatings.

242

243 Figure 4. Relative flux gain by the first meter of guide in the SNS core vessel, as
244 compared to the same EQ-SANS optics with the core vessel guide removed.

245

246 Figure 5. Relative neutron transmissions of four alternative bender configurations with
247 either different radius of curvature (symbols), or number of channels (lines), as compared
248 to the EQ-SANS optics.

249

250 Figure 6. Relative transmission of alternative optical coatings as compared to the EQ-
251 SANS optics. The dashed line is the transmission of Ni coated EQ-SANS optics ($1 \times \theta_c$)

252 versus that of the actual optics. The solid line is when the convex side of the bender is
253 coated with $3.5 \times \theta_c$ supermirrors as well (see text for discussion).

254

255 Figure 7. Integrated flux between the wavelength of 2 and 10 \AA for different beam heights.
256 The width of the optics is held at 40 mm. The $40 \times 40 \text{ mm}^2$ collimation slit and the
257 $20 \times 20 \text{ mm}^2$ sample slit remain in place for all simulations. The flux drops at larger guide
258 heights because when it reaches the height of the SNS moderator (120mm, [3]).

259

260 Figure 8. Upper: Simulated flux distribution across the neutron beam for 2 \AA neutrons at
261 end of the multichannel beam bender. The garland-reflection is evident from the fact that
262 neutrons are concentrated towards the outer walls of each channel. Lower: At the end of
263 the straight neutron guides 10m from the moderator (figure 1). The simulation was
264 performed with $\pm 5^\circ$ of source divergence, which is enough to over saturate the optics.

265

266 Figure 9. Simulated and measured fluxes on the EQ-SANS diffractometer, scaled to
267 1MW source power of the SNS target station. The red circles are measured flux at the
268 sample position with a 4m collimation length. The measurement was taken by placing
269 various sized pinholes at the sample location and using the EQ-SANS detector with
270 corrections for wavelength dependent detection efficiency (92% at 1.8 \AA [1]) applied. The
271 blue crosses are measured flux at the end of the optics with 0m of collimations. The data
272 were collected using the beam monitor at the end of the optics, which is a low pressure
273 gas detector with a calibrated absorption coefficient of $9 \times 10^{-5} \text{ cm}^{-1}$.

274

Fig 1.

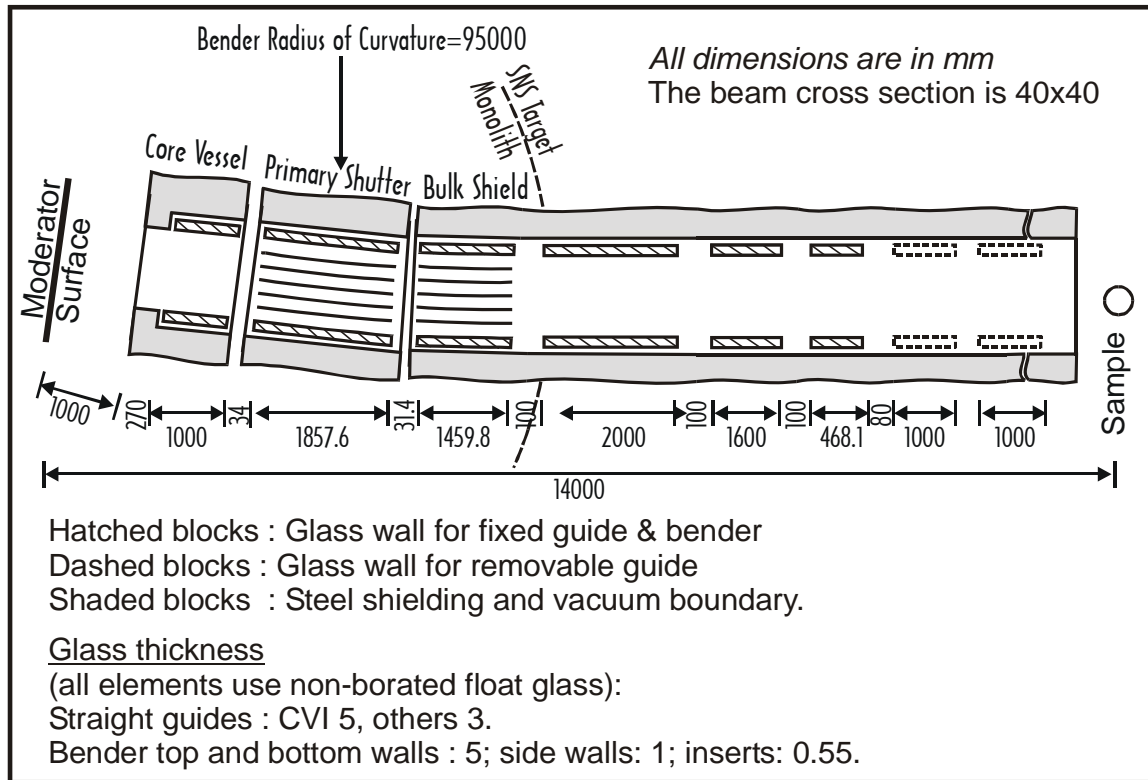


Fig 2.

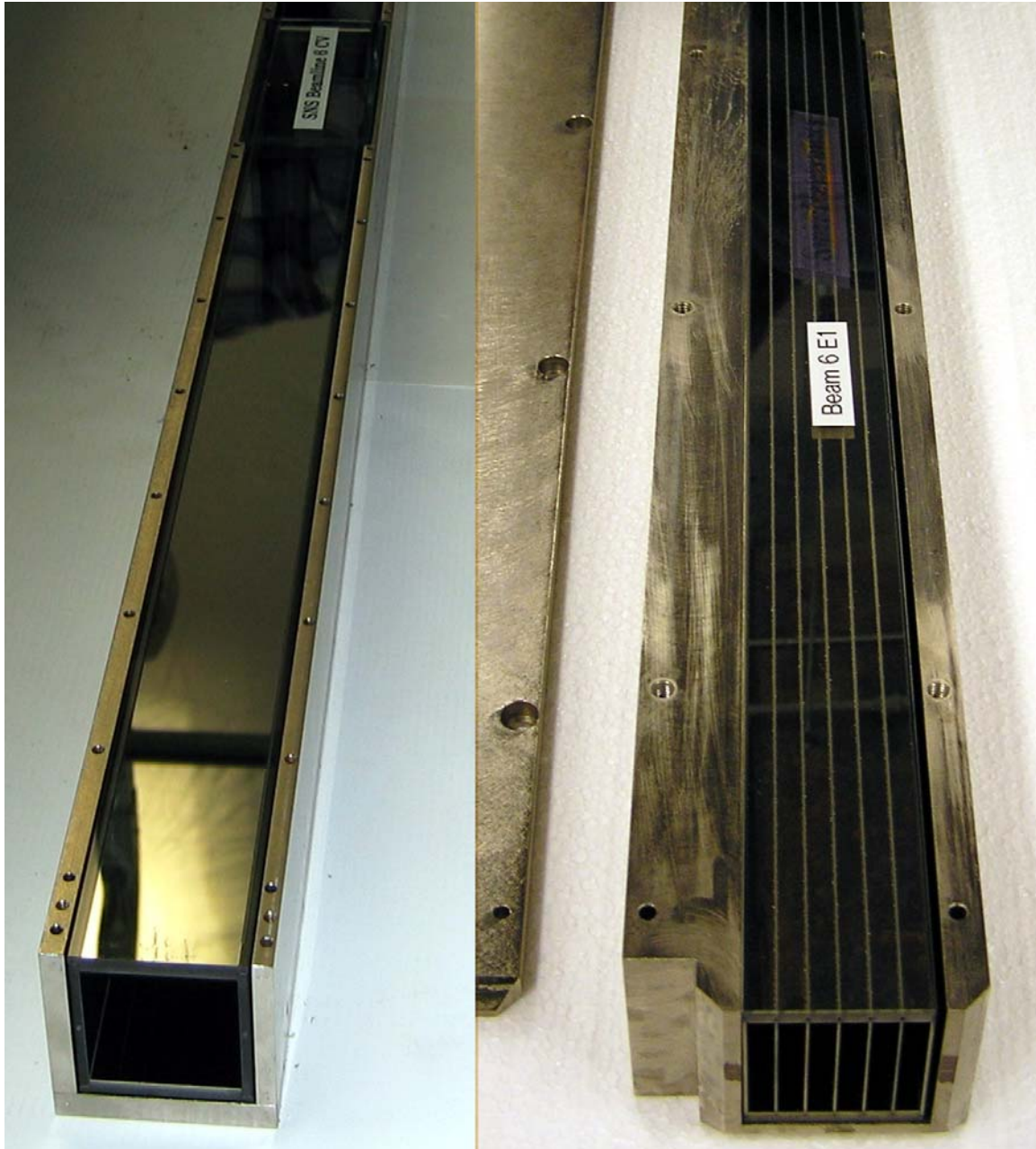


Fig 3.

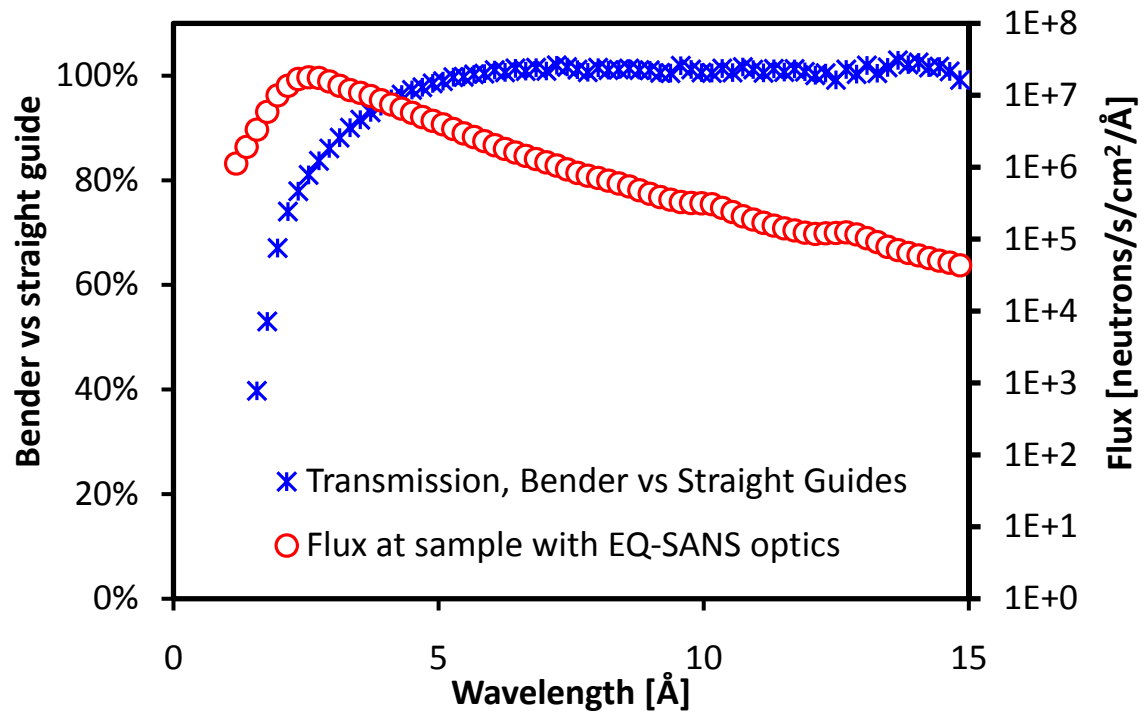


Fig 4.

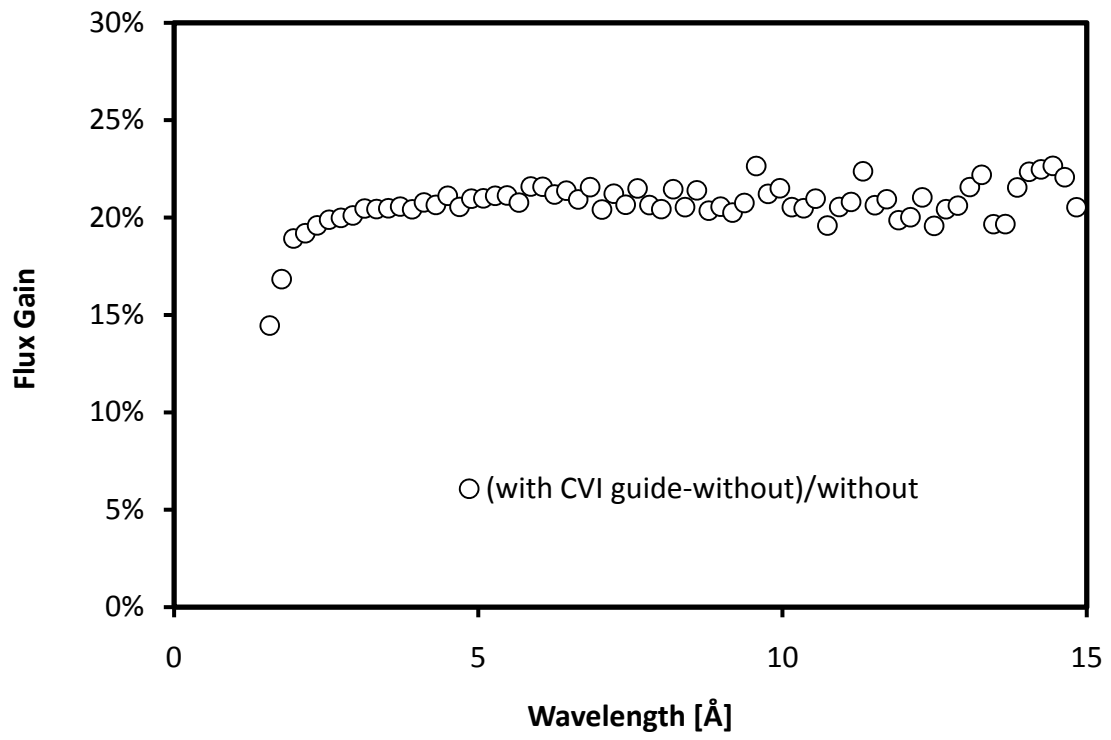


Fig 5

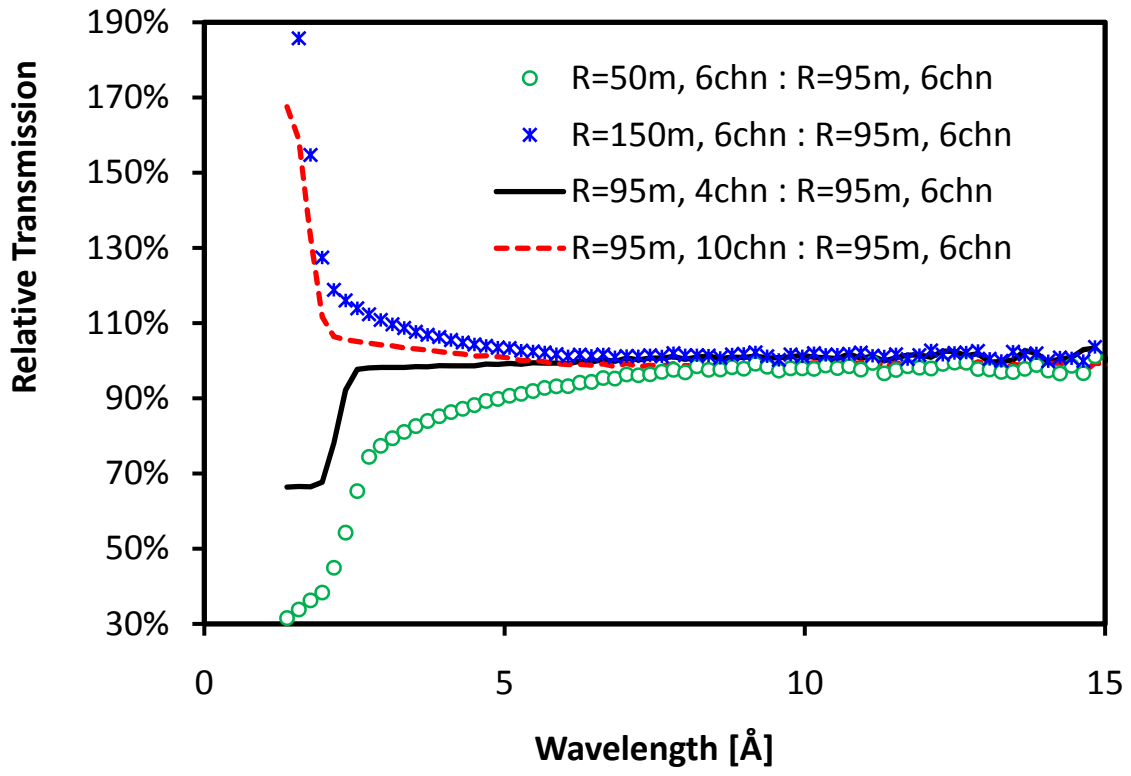


Fig 6

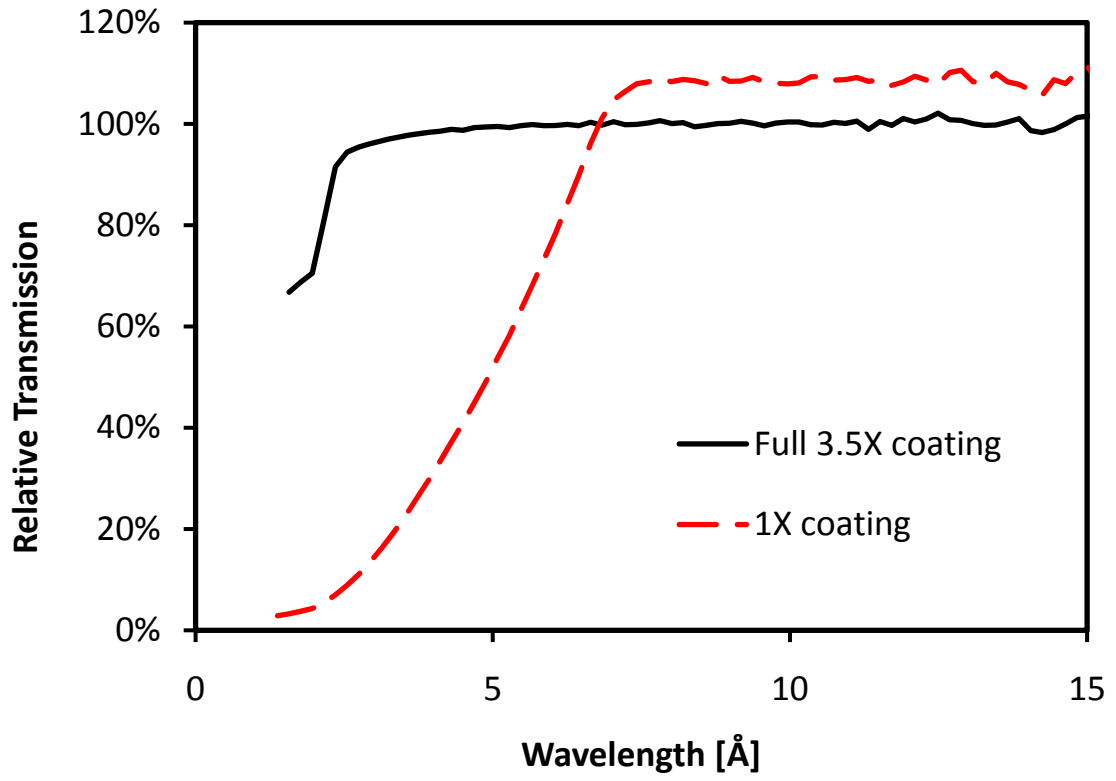


Fig 7

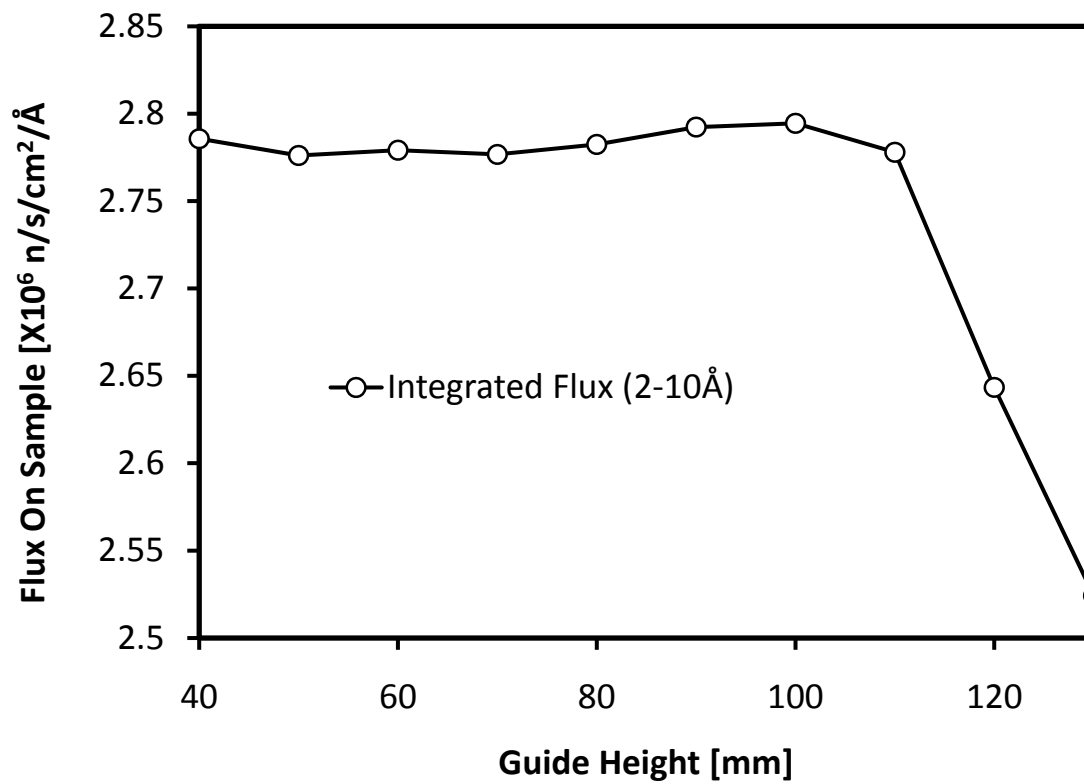


Fig 8

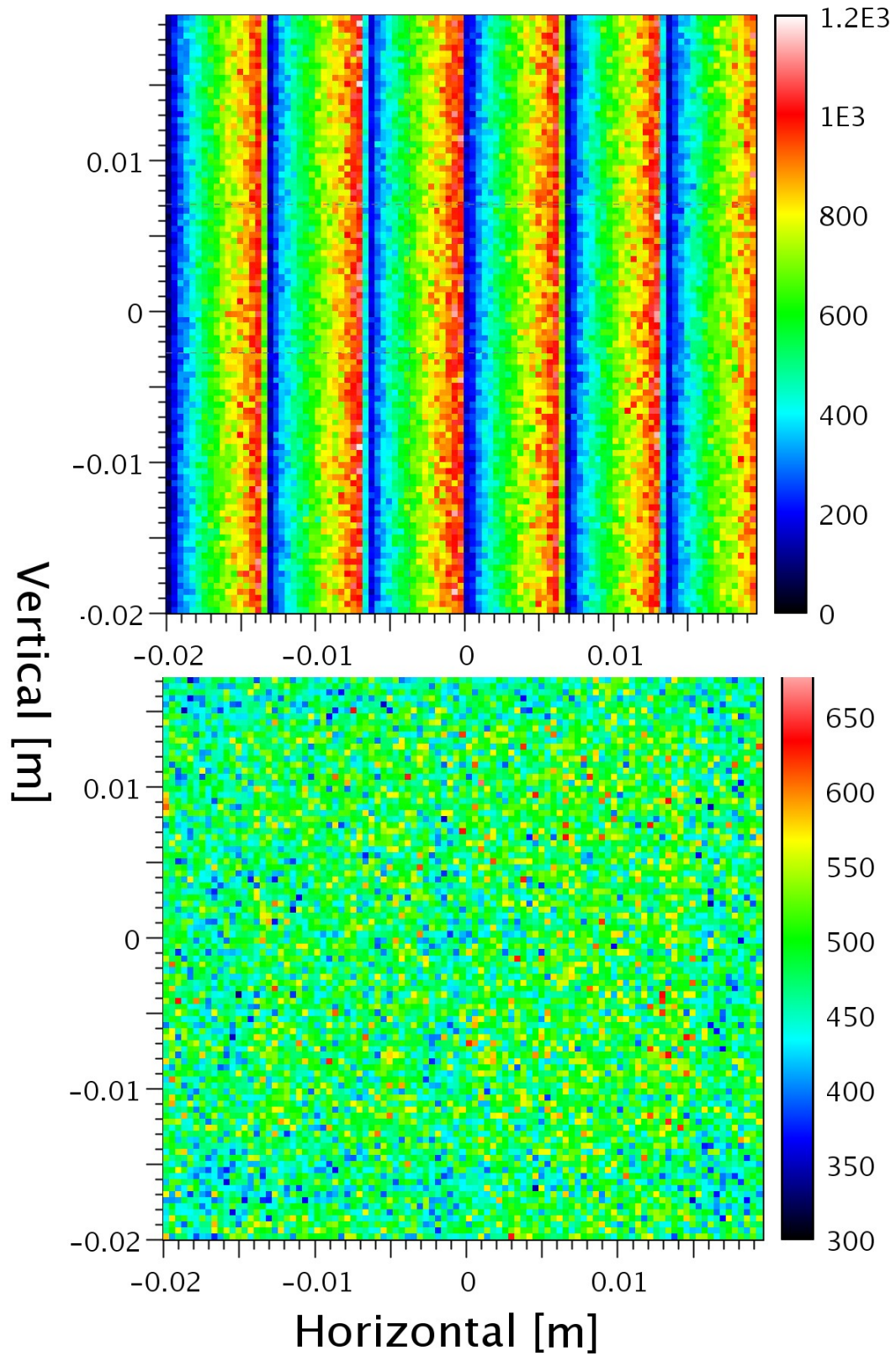


Fig 9

